

# A Skin-Like Hydrogel for Distributed Force Sensing Using an Electrical Impedance Tomography-Based Pseudo-Array Method

Haofeng Chen, Xuanxuan Yang, Jialu Geng, Gang Ma,\* and Xiaojie Wang\*



Cite This: *ACS Appl. Electron. Mater.* 2023, 5, 1451–1460



Read Online

ACCESS |

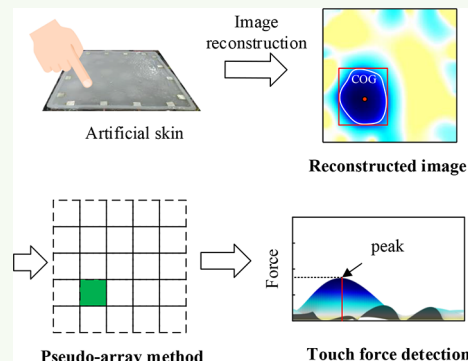
Metrics & More

Article Recommendations

Supporting Information

**ABSTRACT:** Hydrogels are compliant biomaterials that can be integrated with robotic systems to act like human skin for sensing and perception during interactions with their environments. The conventional method for fabricating skin-like hydrogel sensors is based on an array-type design which contains numerous discrete sensitive elements to obtain touch locations and force information. Array-based sensors are complex, with tiny communication units that make manufacturing complicated and expensive. Electrical impedance tomography (EIT) is a noninvasive imaging technique that can be easily implemented to create large-area tactile sensors into a “one-piece” structure without any internal wires. However, EIT-based tactile sensors suffer from low spatial resolution and sensitivity in areas far from the electrodes. This paper introduces a pseudo-array method to remedy the effect of location-dependent sensitivity on the spatial sensing of EIT-based hydrogel sensors and improve their performance for practical applications in detecting distributed contact forces without any arrays or internal wires. As a preliminary study, a skin-like hydrogel-based tactile sensor with an area of 400 cm<sup>2</sup> was fabricated using a simple manufacturing process. The entire piece of the tactile sensor is then divided into a 5 × 5 array, which is referred to as a pseudo-array for simulation and experimental calibration. Each “pseudo-array” unit was calibrated to obtain the mapping relationship between the force and the reconstructed conductivity. Subsequently, a quantitative relationship between the touch force and the EIT measurement for the hydrogel-based tactile sensor for continuous sensing was achieved. Finally, the real-time performance of the EIT-based hydrogel sensor demonstrates that the proposed pseudo-array method can realize more accurate force detection with an error of 1.62 N (10.15% of the maximum force) for sensing distributed force over a large area of 400 cm<sup>2</sup> with only 16 boundary electrodes.

**KEYWORDS:** hydrogel, electrical impedance tomography, pseudo-array method, distributed force sensing, skin-like electronics



## 1. INTRODUCTION

Inspired by the flexible properties and sensing functions of human skins, a variety of skin-like electronics have been explored for the next-generation robotics.<sup>1–3</sup> The robot's bodies covered with these devices are capable of sensing and perception during interactions with their surroundings. Hydrogels as one of compliant biomaterials have shown promise for the skin-like electronic devices owing to their unique properties in stretchability and ionic sensing capability. Hydrogels are formed by cross-linking polymer chains such as physical, ionic, or covalent interactions capable of absorbing large amounts of water. The mobile ions dissolved in the water enable hydrogels to convert external forces/stimuli into electrical signals, making them suitable for sensing.<sup>2,4</sup> To ensure the skin-like hydrogel sensors seamlessly cover complex three-dimensional robotic surfaces and allow robots to perceive external stimuli, such as touch force or pressure, in an unstructured environment, the whole-body devices for distributed tactile sensing are highly demanded.<sup>5–7</sup> The conventional method for the distributed contact-force sensing system is based on an array-type design which contains

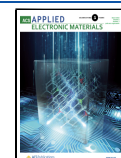
numerous discrete sensitive elements to obtain touch locations and force information.<sup>4,8–10</sup> For example, a four-by-four arrayed sensor based on conductive hydrogels was developed to detect the location and the distribution of an external pressure for practical applications in health monitoring and human/machine interfaces.<sup>4</sup> However, the array-type sensors have inherent disadvantages in their complicated internal wiring and extremely low resolution, especially in large area tactile sensors, and the cost and manufacturing complexity inevitably limit their applications in practice.

Recently, a nonarray tactile sensing technology based on electrical impedance tomography (EIT) has been proposed to overcome the limitations of conventional sensing arrays.<sup>11,12</sup> EIT is a noninvasive imaging technique that allows for

Received: October 12, 2022

Accepted: February 21, 2023

Published: March 1, 2023



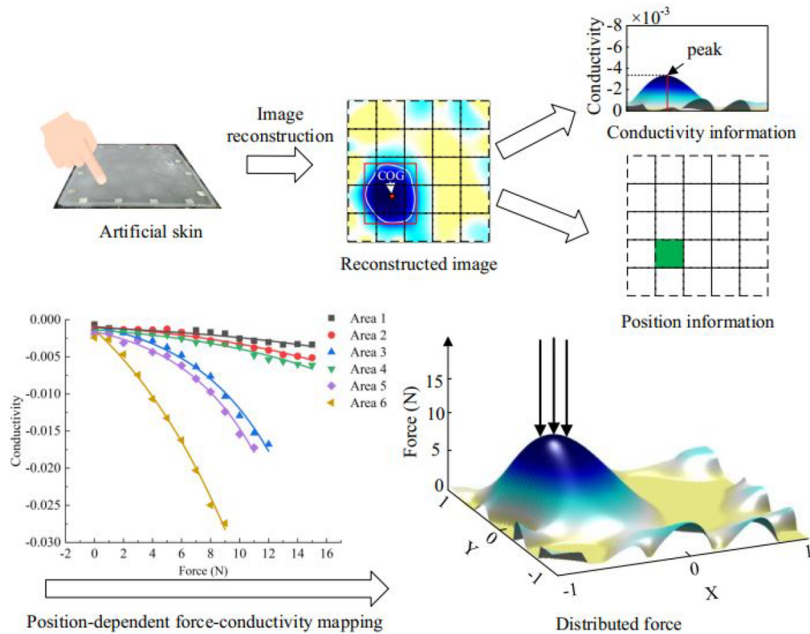


**Figure 1.** Overview of the pseudo-array skin-like tactile sensor.

reconstructing the internal conductivity distribution of a conductive object by processing measurements from boundary electrodes. The measurements are usually carried out through injecting stimulation current between two electrodes and measuring the potentials at the remaining boundary electrodes.<sup>13</sup> As a well-established electrical detection technique, EIT has been proposed for making skin-like hydrogel as a distributed tactile sensor in a “one-piece” structure.<sup>1,14</sup> The EIT-based hydrogel sensor shows low fabrication cost and simple structures with a small number of electrodes which can be easily deployed in a large-area without any internal wires.

In realization of a skin-like hydrogel-based sensor using the EIT technique, it is necessary to provide two-dimensional mapping of the conductivity versus external stimulus such as forces or pressures for the entire sensing area, where the contact location and magnitude should be known. However, due to the ill-posed nonlinear inverse problem of the EIT reconstruction,<sup>13</sup> EIT-based tactile sensors suffer from low spatial resolution and sensitivity in areas far from the electrodes.<sup>14,15</sup> Therefore, some strategies have been proposed to address the issues of spatial resolution and the location-dependent sensitivity in these devices.<sup>11</sup> For example, Tawil et al. added multiple internal electrodes inside the sensing domain to increase the sensitivity of the central region, thereby improving the quality of the reconstructed image.<sup>16</sup> Park et al. proposed a deep neural network based on EIT reconstruction framework and obtained improved spatial resolution, sensitivity, and localization accuracy.<sup>12</sup> Chen and Liu<sup>17</sup> were one of the first to investigate the location-dependent spatial performance of EIT-based tactile sensors. They developed an intensity scaling method to correct reconstructed amplitudes with respect to the uniform sensitivity distribution. Their method can better interpret the strength information on tactile force applied at different positions. However, their method is limited to circular surfaces because they need to divide the entire sensing area into M concentric circles for obtaining scaling values. When the symmetry of the sensing area is not considered, the pseudo-

array method can work normally only by fitting all divided areas and is not limited by the geometric shape of the sensing area. Moreover, the authors of ref 17 verified the feasibility of their method but did not give an example of how to use their system for distributing force measurement. The method we proposed directly established the mapping relationship between the imaging peak and the touch force, so it can be used to estimate the magnitude of the force in the whole sensing area.

In this paper, we proposed a pseudo-array method to remedy the effect of location-dependent sensitivity on the spatial sensing of EIT-based hydrogel sensors so that they can detect distributed contact forces without any arrays and internal wires. First, a simulation study was carried out to illustrate the principle of the proposed tactile sensor where the surface of the sensor is virtually divided into 6 areas for image reconstructions, and the mapping relationship between the force and the reconstructed conductivity is established for each “array unit”. Then, a skin-like hydrogel-based tactile sensor with an area of  $400 \text{ cm}^2$  was fabricated through a simple manufacturing process to validate the proposed pseudo-array method. A customized tactile sensing data acquisition circuit was designed for acquiring impedance data. At last, a quantitative relationship between the touch force and EIT measurement for the hydrogel-based tactile sensor for continuous sensing was evaluated experimentally. Our contributions are as follows.

A nonarray flexible sensing technique providing real-time contact force detection with hydrogel material is proposed. A pseudo-array approach that can reduce the position dependence of EIT-based tactile sensors is investigated. Our work creatively turns a “one-piece” tactile sensor into a “discrete” array tactile sensor to obtain consistent force detection, which greatly increases the practicality of the EIT tactile sensor.

## 2. METHOD

Figure 1 depicts an overview of the proposed pseudo-array skin-like tactile sensing system. The double-network hydrogel is employed to convert force load into impedance conditions due to its similar

mechanical properties of biological tissue, which is suitable for fabricating artificial skin. A whole piece of the tactile sensor is virtually divided into a  $5 \times 5$  array at the software level. The  $5 \times 5$  array is a typical example to verify the concept of the pseudo-array method, which is in compliance with most of the conventional array designs for similar sensors.<sup>10</sup> Taking into account the symmetry of the tactile sensor, the sensor is divided into 6 areas. Physically, the tactile sensor is still a whole piece. When the force is applied at the “array unit”, the hydrogel tactile sensor will be locally deformed, which results in changes in its local impedance. Then, the EIT imaging algorithm is used to obtain the reconstructed image of impedance distribution. Next, we further extracted information from the reconstructed image: conductivity information and position information to obtain the mapping relationship between the force and the reconstructed conductivity on each array unit separately. In this way, the proposed pseudo-array skin-like tactile sensor can perform like an array-type sensor for distributed force detection but has no internal electrodes and wires in a simple whole-piece structure.

Theoretical backgrounds of the EIT-based tactile sensor are provided in [Appendix A](#). This study employs the one-step Gauss–Newton reconstruction method to solve the EIT inverse problem due to its rapid, real-time imaging. Using temporal difference imaging,<sup>18</sup> the solution to the inverse problem can be calculated using the equation as follows:

$$\delta\sigma = (\mathbf{J}^T \mathbf{W} \mathbf{J} + \lambda^2 \mathbf{R})^{-1} \mathbf{J}^T \mathbf{W} \delta \mathbf{V} \quad (1)$$

where  $\mathbf{J}^T$  is the transpose of the Jacobian matrix  $\mathbf{J}$ ,  $\lambda$  is a scalar hyperparameter value,  $\mathbf{W} = \mathbf{I}$ , and  $\mathbf{R}$  is the regularization matrix.<sup>18</sup> The Newton’s One-Step Error Reconstructor (NOSER) prior<sup>19</sup> is used for calculating the matrix  $\mathbf{R}$ , which can be calculated offline. The one-step Gauss–Newton reconstruction method is less computationally expensive and can achieve fast static EIT compared to iterative methods.<sup>20</sup>

Based on the reconstructed image, the relationship between the touch force  $F$  and the peak of conductivity  $P_t$  in touch area follows:

$$F = f_i(P_t, x_t, y_t), \quad i = 1, 2, \dots, N \quad (2)$$

where  $f_i$  is the mapping function on the  $i$ -th “array unit” and  $x_t$  and  $y_t$  are the coordinates of the center of gravity (COG) of the reconstructed image corresponding to the touch area. According to the touch position information, we can choose the corresponding mapping function to predict touch force.

The details of conductivity peak and position information extraction are shown in [Figure 2](#). The impedance data are obtained from the acquisition board. Then, the one-step Gauss–Newton reconstruction method with the NOSER prior is adopted to reconstruct the distribution of conductivity due to its rapid imaging characteristics. An appropriate threshold can detect most of the visually significant effects. Therefore, conductivity less than 60% of the peak conductivity is filtered. Next, all the connected domains are found using the Regionprops Function (RF) method,<sup>21</sup> and the COG of the connected domains is calculated as the touch position information. Finally, we find the maximum value of conductivity in the connected domains as the peak conductivity information.

**2.1. Pseudo-Array Method for Distributed Force Sensing.** **2.1.1. Location-Dependent Performance.** We simulated single-point indentations along the  $x$ -axis direction of a square sensing area to investigate the spatial performance of EIT-based tactile sensors. The local impedance of the sensing materials, e.g., hydrogel used in this study, is changed under indentation. To simplify the simulation, a circular object with a radius of 0.1 relative to a square sensing area (side length = 2) was selected to mimic the indentation. The amplitude of a touch force was modeled as a percentage of the sensor’s background conductivity  $C_0$ . We show a typical example to investigate the spatial performance of EIT-based tactile sensors when  $0.5C_0$  is used to simulate the force applied with a 50% change in local impedance, which is accessible in real applications. The background conductivity of the sensor area is set to 1 S/m. The location-dependent performance was obtained by placing indentations with

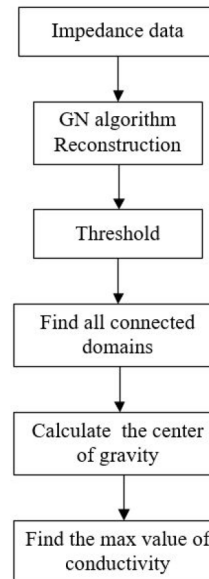


**Figure 2.** Flowchart of conductivity peak and position information extraction.

identical strength along the  $x$ -axis direction, each of the two were separated by a distance of 0.1. [Figure 3a](#) depicts the finite element model (FEM)<sup>22</sup> where the indentation is respectively placed at different positions along the  $x$ -axis direction. [Figure 3b](#) shows the reconstructed images corresponding to the three indentations using Newton’s one-step error reconstructor algorithm. The hyperparameter  $\lambda$  is critical to EIT reconstructions, and the impact of  $\lambda$  on spatial performance has been investigated in ref [17](#). In this study, a moderate hyperparameter  $\lambda = 0.1$  was used. The reconstruction procedure is implemented by the open source code EIDORS.<sup>22</sup>

The conductivity peak of the image is employed to quantify the strength of an unknown touch force according to ref [17](#), because the value in the reconstructed image indicates the conductivity change due to touch strength. The quantitative analysis is shown in [Figure 3c](#), which presents the profiles for the conductivity peak value along the  $x$ -axis direction. As expected, the conductivity peak value of the reconstructed image near the center of the sensor area is the smallest, and the closer to the edge of the sensor, the greater is the conductivity peak value. This is because the distribution of the sensitivity to intensity is nonuniform across the entire sensing area. In order to realize the ability of the EIT tactile sensor to detect the distributed force over the entire sensing area, one can scale the sensitivity matrix. However, the correction method is difficult to implement for sensing areas with arbitrary shapes. Therefore, we propose a pseudo-array method by dividing the sensing area into multiple array units at the software level and establish the relationship between contact force and conductivity at each “array unit” separately.

**2.1.2. Pseudo-Array Method.** To overcome the location dependency of imaging sensitivity of the tactile sensor, a whole piece of the tactile sensor is divided into a  $5 \times 5$  array virtually as shown in [Figure 4a](#). Lo Preti et al. proposed a virtual grid approach for reconstruction of a pressure map in a multitouch soft optical waveguide skin (MSOWS) for multitouch detection.<sup>23</sup> A division into a  $16 \times 16$  grid is used for generating the pattern-recognition-based contact map, and each grid corresponds to the pixel of the pressure map reconstruction, which is similar to the EIT reconstruction using FEM methods which involve the discretization of the domain into smaller grids. However, the proposed pseudo-array method is a postprocessing step in EIT reconstruction which is fundamentally different with the virtual grid approach in ref [23](#). Taking into account the symmetry of the sensor, the sensing area is further divided into six areas, which are represented by six different colors. Physically, the tactile sensor is still a whole piece. In each subarea, we used a circular object with a radius of 0.1

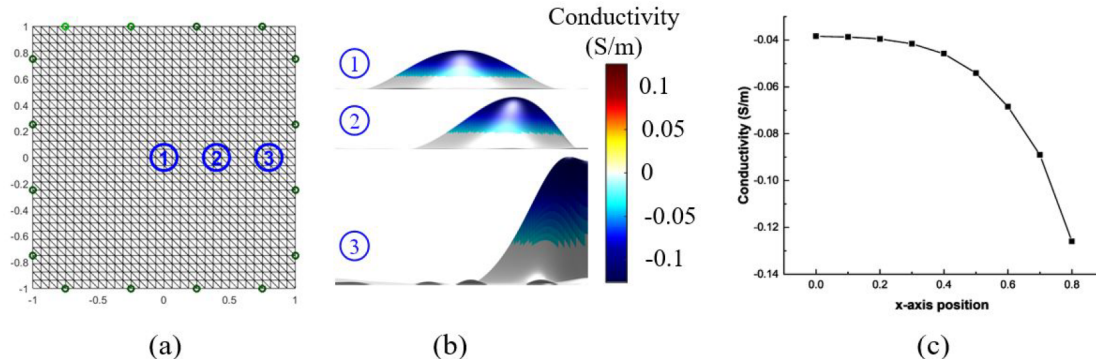


**Figure 3.** Position dependence of the reconstructed conductivity on the EIT-based tactile sensor in simulation. (a) Three objects with the same conductivity and the same size are placed in three different positions. (b) The reconstructed images corresponding to the three objects use the same EIT imaging algorithm. (c) The profiles for peak conductivity along radial directions.

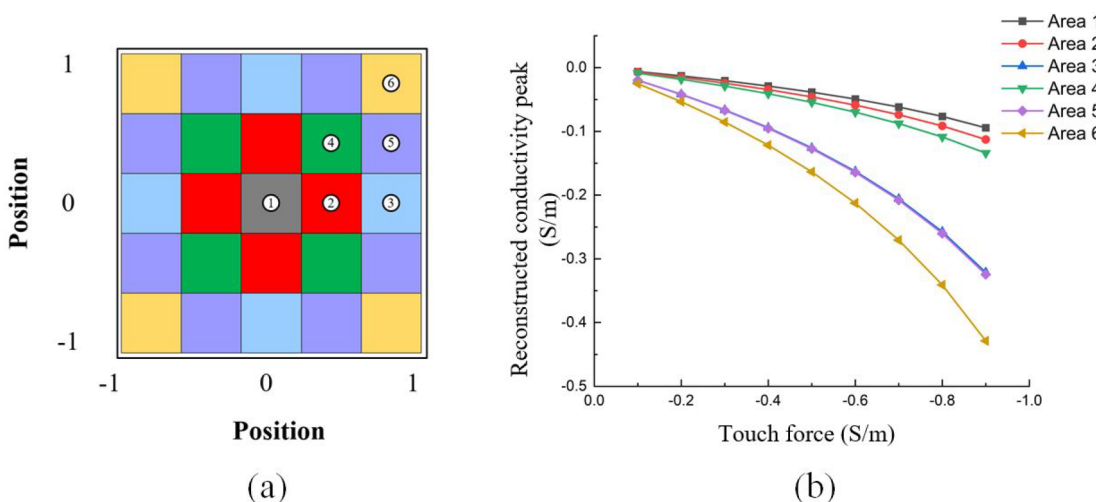


**Figure 4.** Illustrations of the proposed pseudo-array method. (a) Schematic diagram of the sensor area division. (b) The relationship between touch force and reconstructed conductivity peak in different regions.

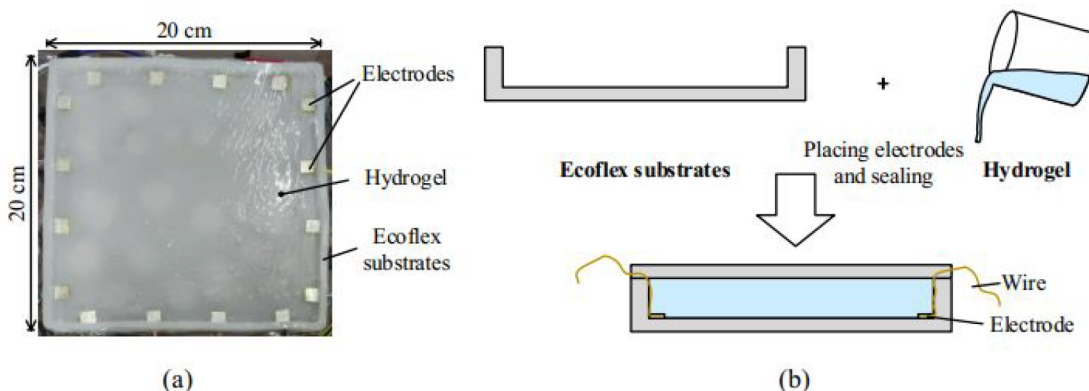


**Figure 5.** Overview of the proposed pseudo-array skin-like tactile sensor. (a) The proposed tactile sensor. (b) The fabrication procedure of hydrogel-based skin-like tactile sensor.

relative to a square sensing area (side length = 2) to mimic the indentation for applying the touch force. The strength of a touch force was modeled as a percentage of the sensor's background conductivity  $C_0$ . In practice, when an external force is applied to the sensor, the local conductivity will decrease. Therefore, in the simulation, we set the conductivity at the contact location to vary from  $0.9C_0$  to  $0.1C_0$  S/m, which is equivalent to a change in conductivity from  $-0.1C_0$  to  $-0.9C_0$  S/m. The one-step Gauss–Newton reconstruction method with the NOSER prior is adopted to reconstruct the distribution of

conductivity. Then, the conductivity peak and position information is calculated. Figure 4b shows the relationship between the simulated touch force and the reconstructed conductivity peak in the six areas, which can be well represented by an exponential function:

$$\hat{\sigma} = a \times e^{(-1/b \times \sigma)} + c \quad (3)$$

where  $a$ ,  $b$ , and  $c$  are constant coefficients and  $\sigma$  and  $\hat{\sigma}$  are real conductivity and reconstructed conductivity, respectively. The average  $R$  squared value is 0.99. From Figure 4b, we can see that, although the

conductivities are the same, the absolute value of the reconstructed conductivity is larger for the areas closer to the electrodes, which indicates that the sensitivity is higher for the areas closer to the electrodes and lower for the areas closer to the center. In addition, we also found that the fitted curves of area 3 and area 5 approximately overlap, indicating that the sensitivity of these two areas is very close.

### 3. EXPERIMENTAL STUDIES

#### 3.1. Tactile Sensor Fabrication and Sensing System.

Figure 5a shows the overview of the proposed pseudo-array skin-like tactile sensor, which was made of a hydrogel with a double-network (DN) cross-linked structure,<sup>14</sup> a soft silicone rubber material Ecoflex (Smooth-on, shore 00–30), and boundary electrodes. Figure 5b shows the sensor fabrication procedure. To prepare the hydrogel, 56.8 g of acrylamide, 6.048 g of acrylic acid, and 0.064 g of methylenebis-(acrylamide) were dissolved in 400 mL of distilled water. Then, 0.8 g of ammonium persulfate and 0.155 g of tetramethylethylenediamine were added, respectively. After thorough mixing, the gel solution was poured into an Ecoflex substrate with sixteen silver evenly attached to the boundary of it to form a tactile sensor with a size of 200 mm × 200 mm × 10 mm. Next, it was put into an oven and kept at 60 °C for 4 h, and then, a hydrogel-based skin-like tactile sensor was obtained (Video S1). Hydrogels exhibit very different properties (mechanical and electrical) as they dehydrate. Therefore, different strategies to enhance the antidehydration capability of hydrogels have been proposed.<sup>2</sup> Zhao et al.<sup>24</sup> used an external packaging strategy for fabricating sandwich-like packaged hydrogel strain sensors to avoid the water loss by evaporation. In this study, we used Ecoflex to encapsulate the hydrogels to prevent the fluctuation of water content. The detailed preparation of skin-like hydrogel is described in the Supporting Information, as shown in Figure S1. The characterizations of skin-like hydrogel are described in the Supporting Information, as shown in Figures S2, S3, and S4.

The overall block diagram of the sensing system of the proposed tactile sensor is illustrated in Figure 6. It mainly

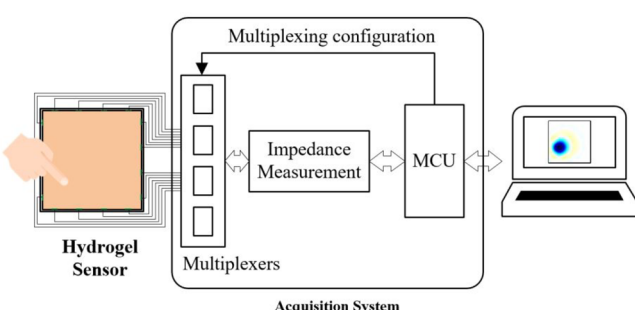


Figure 6. Block diagram of the sensing system.

consists of three parts: hydrogel sensor, acquisition system, and a laptop. The acquisition system includes a Micro Control Unit (MCU), an impedance measurement module, and multiplexers. It is designed to obtain the impedance data from the hydrogel sensor cyclically and send the measured data to a laptop via serial port. The reconstructed algorithm built in the laptop is used to reconstruct the conductivity images.

A customized tactile sensing data acquisition circuit was designed (see Figure 7). A high precision, ultralow power, analog front-end system impedance measurement chip AD5940 is used, which can generate an excitation signal

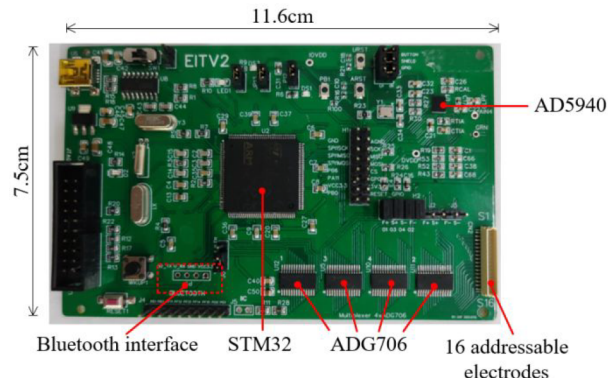


Figure 7. Data acquisition board.

from DC to 200 kHz AC and measure high bandwidth signals up to 200 kHz.<sup>25</sup> In this study, a constant excitation signal of 40 kHz is selected which is used in many EIT systems.<sup>26–28</sup> Four 16-to-1 multiplexers ADG706 are included in our data acquisition board. Two of them connect the current injection terminal to any two electrodes, forming the current-injection pairs. Two more of them connect the voltage-measurement terminals to two electrodes to make up the voltage-measurement pair. In the two-terminal sensing scheme, the current-injection pair is the same as the voltage-measurement pair. In the four-terminal scheme, the current-injection pair is different from the voltage-measurement pair. The four-terminal needs more time to collect data, which limits the real-time imaging capabilities of this system. Therefore, the two-terminal scheme is selected due to its simplicity and high speed. The total loop rate of the proposed tactile sensor is about 1.3 frames/s. The impedance data between all electrode pairs were measured sequentially without repetition, which resulted in 120 independent values (with 16 electrodes). Moreover, the microcontroller STM32 is employed for controlling the multiplexer to connect the AD5940 and 16 addressable electrodes and sending the processed impedance data from AD5940 to a computer. More design details can be found in our previous paper.<sup>29</sup>

**3.2. Experimental Setup and Procedure.** The experimental apparatus for validating the proposed pseudo-array skin-like tactile sensor is shown in Figure 8. A universal testing machine (E44.104, MTS, US) equipped with a linear actuator and a 100 N load cell is employed. A plastic cylindrical indenter with a diameter of 20 mm is used to apply touch

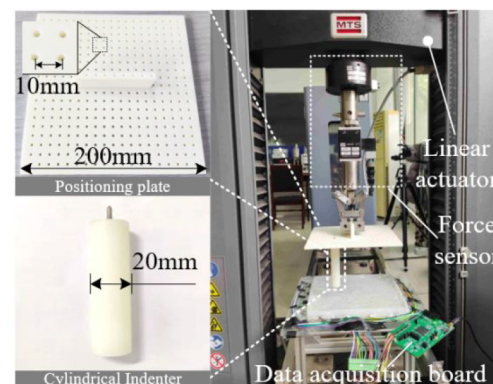
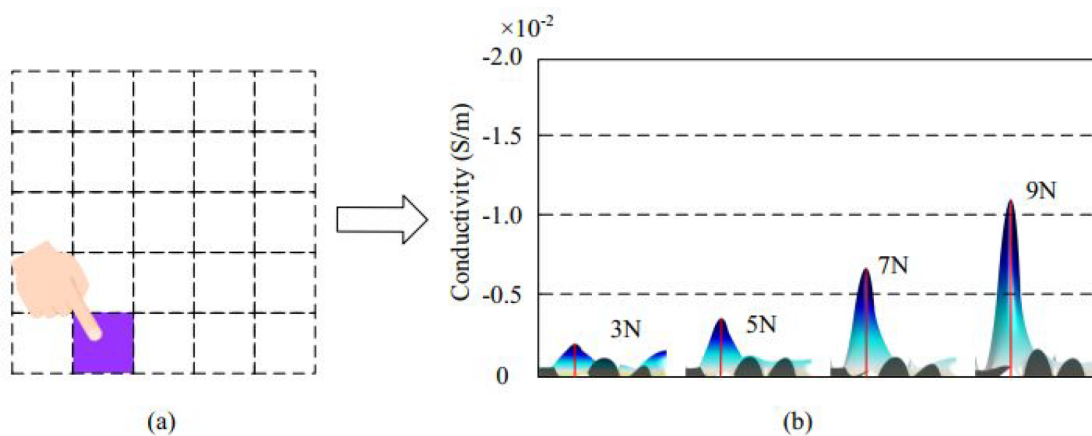


Figure 8. Experimental apparatus for evaluating the tactile sensor performance.

**Table 1. Results of Touch Detection Experiments**

	Touch	Reconstructed image	Thresholding	Touch position information
Touch				Touch position: (0.45, 0.01) Touch Area: 1
Reconstructed image				Touch position: (-2.27, 1.27) Touch Area: 2
Thresholding				Touch position: (-7.98, -0.07) Touch Area: 3
Touch position information				Touch position: (-3.29, -3.32) Touch Area: 4
				Touch position: (-4.54, -8.74) Touch Area: 5



**Figure 9.** Reconstructed conductivity peak with different loads in the same area. (a) Schematic diagram of the touch position. (b) Three-dimensional reconstructed image obtained by applying different loads (front view).

force. A 200 mm × 200 mm positioning plate with 19 × 19 holes is used to fix the indenter and connected to the MTS load cell through a metal clamp.

**3.3. Evaluation of Pseudo-Array Method.** To better illustrate the touch location detection capability, we make a comparison between the experimental EIT images and the predicted localization on the  $5 \times 5$  grid. Table 1 presents five representative results of touch detection experiments with the same load of 10 N applied in different areas. We obtain a preliminary reconstructed image through the EIT reconstruction algorithm. Then, we calculate the coordinates of the touch location and the area to which it belongs after thresholding. As can be seen, the position information effectively obtained reflects the location of the touch. The localization performance

of the tactile sensor is described in the Supporting Information, as shown in Figure S5.

We further explored the force detection performance of the tactile sensor under different pressing forces. Figure 9 shows the result of the reconstructed peak conductivity with different loads in the same area. Figure 9a shows the schematic diagram of the touch position, and Figure 9b presents the three-dimensional reconstructed image obtained by applying different loads. As can be seen, the conductivity peak of the reconstructed image increases with increasing load, which illustrates that the proposed tactile sensor based on hydrogels can effectively detect the force load.

Figure 10 presents the reconstructed conductivity peak with the same load applied in different areas. Due to the location

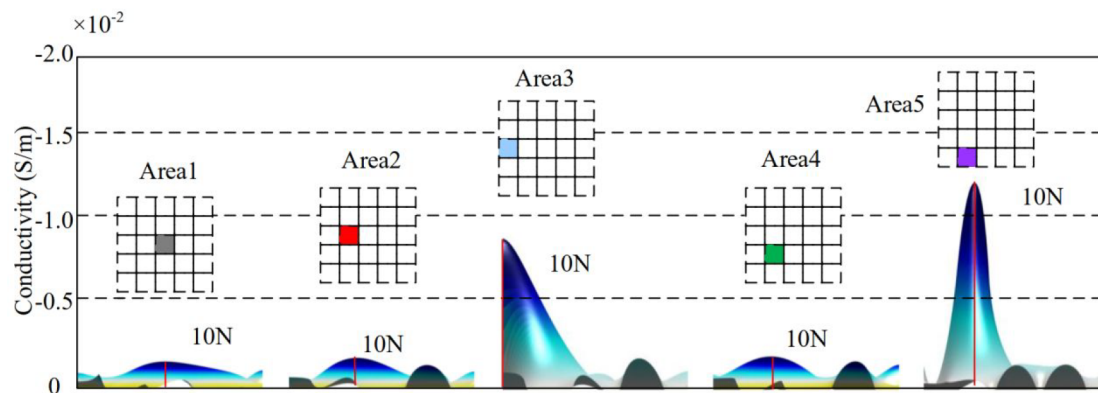


**Figure 10.** Reconstructed peak conductivity with the same load applied in different areas.

dependency of the EIT-based tactile sensor, the same loads in different areas result in different imaging conductivity peak values. We compared the reconstructed images with a force of 10 N applied to each of the different areas, and as expected, the conductivity peak value in the array unit near the edge was significantly larger than that in the center area.

The relationship between load force and reconstructed conductivity peak in different areas in the experiment is

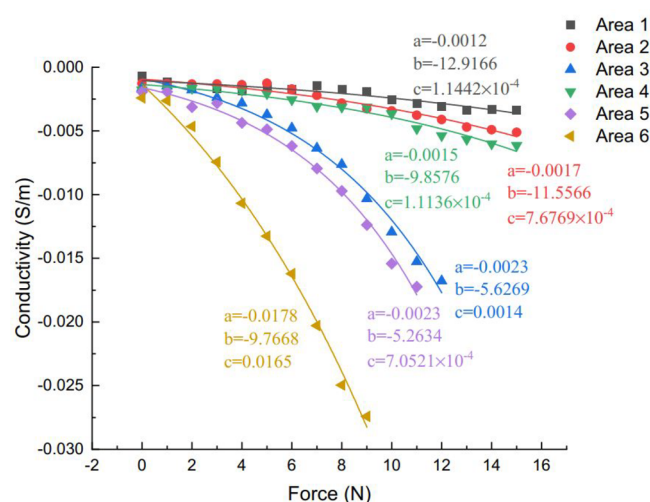


**Figure 11.** Relationship between load force and reconstructed conductivity in different regions in experiment.

presented in Figure 11, which is consistent with the simulation results and can also be represented by an exponential function:

$$\sigma(F) = a \times e^{(-1/b \times F)} + c \quad (4)$$

where  $a$ ,  $b$ , and  $c$  are constant coefficients,  $\sigma$  is reconstructed conductivity, and  $F$  is load force. According to the result of simulation, we divided the sensing area of the tactile sensor into six areas (Figure 4) with 25 individual array units. In the  $3 \times 3$  grid area in the lower left corner of the sensor area, the fitting data set is collected. In the  $3 \times 3$  grid area in the lower right corner and the upper right corner of the sensor area, the validation data set is collected. The central areas 1, 2, and 4 are far from the electrodes, where the sensitivity is very low, and a larger force is needed than in the edge area to get stable imaging. Therefore, we acquired data in the central area (1, 2, 4) with a force loading range of 0–15 N at an interval of 1 N.

The force loading range in area 3 was 0–12 N; the force loading range in area 5 was 0–11 N; the force loading range in area 6 was 0–9 N; the intervals of the loading forces were all 1 N. To simplify the experiment and considering the geometric symmetry of the tactile sensor, we selected a representative array unit on each of the six areas to collect data for training and later collected data on other areas for validation. Up to 15 time series samples were recorded, and the data were used to reconstruct images for one touch test. A total of 1245 samples were collected for fitting the relationship between touch force and reconstructed electrical conductivity peak. The best-fit values of  $a$ ,  $b$ ,  $c$  and the corresponding  $R^2$  squared values for the exponential functions in six different areas are presented in Table 2. As can be seen, in the center areas (area 1, area 2, and

**Table 2. Best Fitting Parameters and  $R^2$  Squared Values**

area	$a$	$b$	$c$	$R^2$
1	-0.0012	-12.9166	$1.1442 \times 10^{-4}$	0.89
2	-0.0017	-11.5566	$7.6769 \times 10^{-4}$	0.96
3	-0.0023	-5.6269	0.0014	0.98
4	-0.0015	-9.8576	$1.1136 \times 10^{-4}$	0.96
5	-0.0023	-5.2634	$7.0521 \times 10^{-4}$	0.99
6	-0.0178	-9.7668	0.0165	0.99

area 4), the values of the reconstructed conductivity peak are closer to each other and gradually separated as the force increased. It indicates that the sensitivity of the EIT-based tactile sensors is lower at the center, especially for the small forces. In the edge areas (area 3, area 5, and area 6), the changes of the reconstructed conductivity with the applied forces are significant, but they are saturated quickly. For example, in area 6, the sensor can only measure up to 9 N, then no more or less change occurs when force increases. In practice, we first obtain the peak conductivity based on the reconstructed image. At the same time, the area where the touch force is located is determined according to the coordinate of the touch position. Then, the corresponding fitting parameters are selected for force estimation by solving the inverse function of eq 4. Therefore, this pseudo-array approach might be able to make the skin-like hydrogel tactile sensors sense distributed forces over a large area.

To verify the performance of the pseudo-array sensor, we randomly selected multiple locations (including six regions) outside the fitted data collection area. The force range is from 0 to 16 N, and the magnitude of the force is applied randomly. Over 475 samples were collected in the test. These 475

samples are collected in the  $3 \times 3$  grid area in the lower right corner and the upper right corner of the sensor area, which cover the six areas of the pseudo-array method. Figure 12

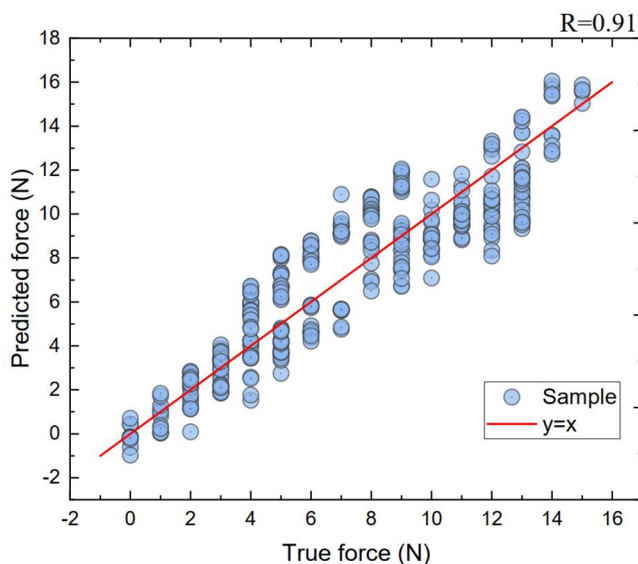


**Figure 12.** Force detection results using the proposed method.

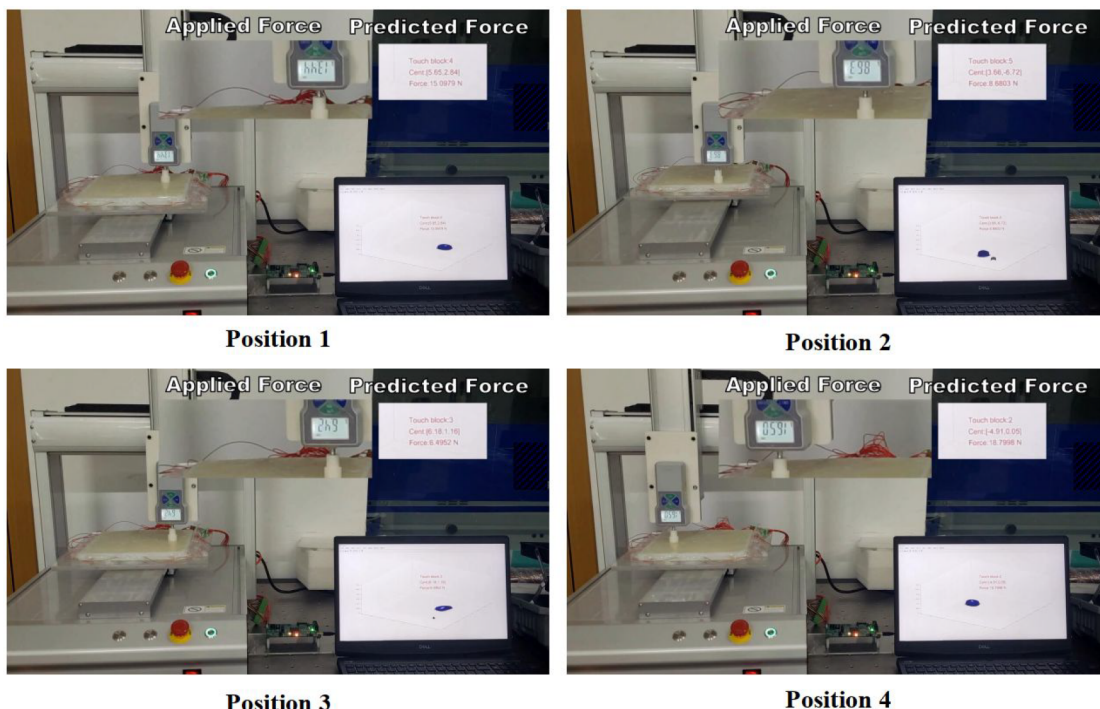
shows the relationship between the true force and the predicted force with a linear correlation coefficient of 0.91, and the RMS value of the calculated force and the real force is 1.62 N (10.15% max force).

Figure 13 shows some examples of real-time touch tests using the proposed pseudo-array sensor (Video S2). We used a XYZ stage equipped with a commercial force gauge (SH-100, NSCING, China) to precisely apply touch force at a specified location. The laptop is used to display the amplitude of the

touch force by a 3-D reconstructed image. The touch position information is shown as the text of Touch block and Cent. Touch block represents the area of touch, and Cent is the center position of the touch. The predicted force is presented as text of Force. When we apply random touch force to the sensing areas, the proposed pseudo-array flexible tactile sensor can realize real-time and more accurate force detection, which is practical for whole-body tactile sensing of human–robot interactions.

#### 4. SUMMARY AND CONCLUSION

In this study, we developed a pseudo-array hydrogel-based tactile sensor using the EIT technique, including the design, fabrication, and signal processing of the proposed system. The EIT is a noninvasive imaging technique that can be easily implemented to create large-area tactile sensors, without any internal wires. Hydrogels with good piezoresistive and mechanical properties are applied as the sensing material. Owing to their biomimetic structures and suitable mechanical properties, the proposed skin-like hydrogel sensor has potential for human–machine tactile perception. A pseudo-array method is adopted to reduce the problem of location-dependent sensitivity of the EIT-based tactile sensors. The performance of the proposed method is verified in both simulations and experiments. The performance of the skin-like hydrogel tactile sensor has an error of 1.62 N (10.15% of the maximum force) for sensing distributed force over a large area of  $400 \text{ cm}^2$  with only 16 boundary electrodes. The results indicate that the proposed pseudo-array method is effective in estimating the predicted contact force in the case of single touch, although its accuracy is relatively low. To reduce prediction errors, we can use a finer division of areas and more advanced calibration methods like machine learning. In addition, this method is not limited by the shape of the sensing area and is very simple to implement. However, the



**Figure 13.** Real-time force detection demonstration.

pseudo-array method only realizes single point force detection. Multipoint touch detection is an intrinsic capability of EIT-based reconstruction methods, which can be achieved during the EIT reconstruction stage. However, quantitatively detecting multipoint touch forces is a challenging task. The quantitative relationship between single-point touch force and EIT measurement cannot be easily applied to the detection of multipoint touch force, as the system's measurements during multipoint touches cannot be estimated simply by adding together the measurements made during individual touches. In the future, we will continue to investigate the detection of multipoint touch forces to further enhance the capabilities of tactile sensors.

## APPENDIX

### Theoretical Backgrounds of the EIT-Based Tactile Sensor

We used a finite element model (FEM) method with a complete electrode model<sup>11</sup> to calculate the boundary voltages on the boundary electrodes according to the conductive distribution of the proposed tactile sensor, which is implemented by an open source code EIDORS.<sup>22</sup> Given a conductive domain ( $\Omega$ ) and its boundary ( $\partial\Omega$ ), the relationship between the boundary potential  $u$  and conductivity distribution  $\sigma$  on a steady-state conductivity body  $\Omega$  is subject to the Laplacian elliptic partial differential equation according to Maxwell's equation for electromagnetism

$$-\nabla \cdot (\sigma \nabla u) = 0 \quad \text{on} \quad \Omega \quad (5)$$

with the boundary condition

$$\int_{e_l} \sigma \frac{\partial u}{\partial \mathbf{n}} ds = I_l \quad \text{on} \quad e_l, \quad l = 1, 2, \dots, L \quad (6)$$

$$u + z_l \sigma \frac{\partial u}{\partial \mathbf{n}} = V_l \quad \text{on} \quad e_l, \quad l = 1, 2, \dots, L \quad (7)$$

$$\sigma \frac{\partial u}{\partial \mathbf{n}} = 0 \quad \text{on} \quad \partial\Omega \setminus \bigcup_{l=1}^L e_l, \quad l = 1, 2, \dots, L \quad (8)$$

where  $L$  denotes the number of electrodes,  $e_l$  is the  $l$ -th electrode,  $I_l$  represents the current flowing through the  $l$ -th electrode,  $V_l$  is voltage measurements from the  $l$ -th electrodes,  $z_l$  denotes the contact impedance, and  $\mathbf{n}$  is outward unit vector normal to  $\partial\Omega$ . To ensure the uniqueness of the solution, the conservation of the charge theorem must hold

$$\sum_{l=1}^L I_l = 0, \quad \sum_{l=1}^L V_l = 0 \quad (9)$$

We define a forward operator  $H$  as a map from the conductivity distribution  $\sigma$  to boundary voltage  $\mathbf{V}$  measured from electrodes, that is

$$H(\sigma) = \mathbf{V} \quad (10)$$

The inverse problem of EIT is to recover the change of conductivity  $\delta\sigma$  in the conductive domain  $\Omega$  from the change in boundary voltage  $\delta\mathbf{V}$ . The relationship between  $\delta\sigma$  and  $\delta\mathbf{V}$  can be linearized

$$\delta\mathbf{V} = \mathbf{J}\delta\sigma + \mathbf{n}_{\text{noise}} \quad (11)$$

where  $\mathbf{J}$  is a Jacobian matrix and  $\mathbf{n}_{\text{noise}}$  denotes the measurement noise.

## ASSOCIATED CONTENT

### Supporting Information

The Supporting Information is available free of charge at <https://pubs.acs.org/doi/10.1021/acsaclm.2c01394>.

Preparation of skin-like hydrogel and characterizations; localization performance (PDF)

Hydrogel-based skin-like tactile sensor (MP4)

Real-time touch test video (MP4)

## AUTHOR INFORMATION

### Corresponding Authors

Gang Ma – University of Science and Technology of China, Hefei, Anhui 230026, China; Email: [magang93@ustc.edu.cn](mailto:magang93@ustc.edu.cn)

Xiaojie Wang – The Institute of Intelligent Machines, Hefei Institutes of Physical Science, Chinese Academy of Sciences, Hefei, Anhui 230031, China; [orcid.org/0000-0002-4740-7882](https://orcid.org/0000-0002-4740-7882); Email: [xjwang@iamt.ac.cn](mailto:xjwang@iamt.ac.cn)

### Authors

Haofeng Chen – The Institute of Intelligent Machines, Hefei Institutes of Physical Science, Chinese Academy of Sciences, Hefei, Anhui 230031, China; University of Science and Technology of China, Hefei, Anhui 230026, China

Xuanxuan Yang – The Institute of Intelligent Machines, Hefei Institutes of Physical Science, Chinese Academy of Sciences, Hefei, Anhui 230031, China; University of Science and Technology of China, Hefei, Anhui 230026, China

Jialu Geng – The Institute of Intelligent Machines, Hefei Institutes of Physical Science, Chinese Academy of Sciences, Hefei, Anhui 230031, China

Complete contact information is available at: <https://pubs.acs.org/10.1021/acsaclm.2c01394>

### Notes

The authors declare no competing financial interest.

## ACKNOWLEDGMENTS

This work was supported in part by the Key Support Project of Dean Fund of Hefei Institutes of Physical Science, CAS, under Grant YZJJZX202017; in part by the Fundamental Research Funds for the Central Universities under Grant WK5290000003; in part by the Innovation and Entrepreneurship Fund of Science Island Graduate Innovation and Entrepreneurship Center under Grant KY-2021-SC-03.

## REFERENCES

- Park, K.; Yuk, H.; Yang, M.; Cho, J.; Lee, H.; Kim, J. A biomimetic elastomeric robot skin using electrical impedance and acoustic tomography for tactile sensing. *Science Robotics* **2022**, *7* (67), eabm7187.
- Ying, B.; Liu, X. Skin-like hydrogel devices for wearable sensing, soft robotics and beyond. *Science* **2021**, *24* (11), 103174.
- Sarwar, M. S.; Dobashi, Y.; Preston, C.; Wyss, J. K.; Mirabbasi, S.; Madden, J. D. W. Bend, stretch, and touch: Locating a finger on an actively deformed transparent sensor array. *Science advances* **2017**, *3* (3), e1602200.
- Tai, Y.; Mulle, M.; Ventura, I. A.; Lubineau, G. A highly sensitive, low-cost, wearable pressure sensor based on conductive hydrogel spheres. *Nanoscale* **2015**, *7* (35), 14766–14773.
- Ho, V. A.; Nakayama, S. IoTouch: whole-body tactile sensing technology toward the tele-touch. *Advanced Robotics* **2021**, *35* (11), 685–696.

- (6) Dahiya, R. S.; Valle, M. *Robotic tactile sensing: technologies and system*; Springer: New York, NY, USA, 2013.
- (7) Dahiya, R. S.; Metta, G.; Valle, M.; Sandini, G. Tactile sensing—from humans to humanoids. *IEEE transactions on robotics* **2010**, *26* (1), 1–20.
- (8) Schmitz, A.; Maiolino, P.; Maggiali, M.; Natale, L.; Cannata, G.; Metta, G. Methods and Technologies for the Implementation of Large-Scale Robot Tactile Sensors. *IEEE Transactions on Robotics* **2011**, *27* (3), 389–400.
- (9) Yang, Z. W.; Pang, Y.; Zhang, L.; Lu, C.; Chen, J.; Zhou, T.; Zhang, C.; Wang, Z. L. Tribotronic Transistor Array as an Active Tactile Sensing System. *acs nano* **2016**, *10* (12), 10912–10920.
- (10) Castellanos-Ramos, J.; Trujillo-Leon, A.; Navas-Gonzalez, R.; Barbero-Recio, F.; Sanchez-Duran, J. A.; Oballe-Peinado, O.; Vidal-Verdu, F. Adding Proximity Sensing Capability to Tactile Array Based on Off-the-Shelf FSR and PSoC. *IEEE Transactions on Instrumentation and Measurement* **2020**, *69* (7), 4238–4250.
- (11) Silvera-Tawil, D.; Rye, D.; Soleimani, M.; Velonaki, M. Electrical Impedance Tomography for Artificial Sensitive Robotic Skin: A Review. *Ieee Sens J.* **2015**, *15* (4), 2001–2016.
- (12) Park, H.; Park, K.; Mo, S.; Kim, J. Deep Neural Network Based Electrical Impedance Tomographic Sensing Methodology for Large-Area Robotic Tactile Sensing. *IEEE Transactions on Robotics* **2021**, *37* (5), 1570–1583.
- (13) Holder, D. S. *Electrical Impedance Tomography: Methods, History and Applications*; IOP Publishing: Bristol, U.K., 2005.
- (14) Liu, Z.; Zhang, T.; Yang, M.; Gao, W.; Wu, S.; Wang, K.; Dong, F.; Dang, J.; Zhou, D.; Zhang, J. Hydrogel Pressure Distribution Sensors Based on an Imaging Strategy and Machine Learning. *ACS Appl. Electron. Mater.* **2021**, *3* (8), 3599–3609.
- (15) Sun, X.; Yao, F.; Li, J. Nanocomposite hydrogel-based strain and pressure sensors: a review. *Journal of Materials Chemistry A* **2020**, *8* (36), 18605–18623.
- (16) Tawil, D. S.; Rye, D.; Velonaki, M. Improved image reconstruction for an EIT-based sensitive skin with multiple internal electrodes. *IEEE Transactions on Robotics* **2011**, *27* (3), 425–435.
- (17) Chen, Y.; Liu, H. Location-Dependent Performance of Large-Area Piezoresistive Tactile Sensors based on Electrical Impedance Tomography. *Ieee Sens J.* **2021**, *21* (19), 21622–21630.
- (18) Adler, A.; Dai, T.; Lionheart, W. R. Temporal image reconstruction in electrical impedance tomography. *Physiological measurement* **2007**, *28* (7), S1.
- (19) Cheney, M.; Isaacson, D.; Newell, J. C.; Simske, S.; Goble, J. NOSER: An algorithm for solving the inverse conductivity problem. *International Journal of Imaging systems and technology* **1990**, *2* (2), 66–75.
- (20) Wang, M. Inverse solutions for electrical impedance tomography based on conjugate gradients methods. *Measurement Science and Technology* **2002**, *13* (1), 101–117.
- (21) The MathWorks. *MATLAB Image Processing Toolbox User's Guide*; <http://matlab.izmiran.ru/help/toolbox/images/>.
- (22) Adler, A.; Lionheart, W. R. Uses and abuses of EIDORS: an extensible software base for EIT. *Physiological measurement* **2006**, *27* (S), S25–S42.
- (23) Lo Preti, M.; Totaro, M.; Falotico, E.; Crepaldi, M.; Beccai, L. Online Pressure Map Reconstruction in a Multitouch Soft Optical Waveguide Skin. *IEEE/ASME Transactions on Mechatronics* **2022**, *27* (6), 4530–4540.
- (24) Zhao, M.; Zhang, W.; Wang, D.; Sun, P.; Tao, Y.; Xu, L.; Shi, L. A Packaged and Reusable Hydrogel Strain Sensor with Conformal Adhesion to Skin for Human Motions Monitoring. *Advanced Materials Interfaces* **2022**, *9* (6), 2101786.
- (25) Analog Devices, *High Precision, Impedance, and Electrochemical Front End; AD5940/5941 Data Sheet*; Accessed: 2020; <https://www.analog.com/media/en/technical-documentation/data-sheets/AD5940-5941.pdf>.
- (26) Ma, G.; Hao, Z.; Wu, X.; Wang, X. An Optimal Electrical Impedance Tomography Drive Pattern for Human-Computer Interaction Applications. *IEEE Transactions on Biomedical Circuits and Systems* **2020**, *14* (3), 402–411.
- (27) Zhang, Y.; Xiao, R.; Harrison, C. Advancing hand gesture recognition with high resolution electrical impedance tomography. In *Proceedings of the 29th Annual Symposium on User Interface Software and Technology*; ACM, 2016; pp 843–850.
- (28) Zhang, Y.; Harrison, C. Tomo: Wearable, low-cost electrical impedance tomography for hand gesture recognition. In *Proceedings of the 28th Annual ACM Symposium on User Interface Software & Technology*; ACM, 2015; pp 167–173.
- (29) Chen, H.; Yang, X.; Wang, P.; Geng, J.; Ma, G.; Wang, X. A Large-Area Flexible Tactile Sensor for Multi-Touch and Force Detection Using Electrical Impedance Tomography. *Ieee Sens J.* **2022**, *22* (7), 7119–7129.